The 33rd Conference of The Mechanical Engineering Network of Thailand
2 - 5 July 2019, Udon Thani
HTE – 020

Numerical Simulation of Turbulent Flow and Heat Transfer in Hexagonal Dimpled Channel

Somchai Sripattanapipat[1,*], Satienpong Huyanan[1], Watanyoo Phairote[2] and Pongjet Promvonge[2]

[1] Department of Mechanical Engineering, Faculty of Engineering, Mahanakorn University of Technology, Bangkok 10530

[2] Department of Mechanical Engineering, Faculty of Engineering, King Mongkut's Institute of Technology Ladkrabang, Bangkok 10520

*Corresponding Author: ssomchai@mut.ac.th, +662 988-3666, +662 988-3666

Abstract

The paper deals with a numerical analysis of heat transfer and turbulent flow behaviors in a channel with staggered hexagonal dimples on the lower wall. With Reynolds numbers (Re) ranging from 5000 to 20,000, air flows into the channel having a constant wall heat-flux condition. The computations are based on the method of finite volume using the RNG k-ε turbulence model for closure of the problem. The numerical result shows that the dimpled surface can produce the vortex flow that helps to cause the flow impingement or attachment on the wall regions leading to an increase in the heat transfer rate. Furthermore, the effects of dimple parameters such as relative dimple depth (d/H) on flow and thermal characteristics are examined numerically. The numerical result demonstrates that with the increment of d/H, the heat transfer and friction loss increase. The hexagonal dimpled surface implementation offers the greater thermal performance compared to the smooth channel alone.

Keywords: Hexagonal dimpled channel, Turbulent flow, Heat transfer enhancement.

1. Introduction

In many industrial applications, heat transfer improvement in a channel is of interest and importance. Ligrani et al. [1] compared several kinds of the heat transfer enhancement methods and found that the dimpled surfaces yielded better overall efficiency relative to pin-fins, rib turbulators and other surface roughnesses. Xia et al. [2] numerically examined the increase in heat transfer with pins, dimples or protrusions on a turbine blade tip wall. Elyyan and Tafti [3] showed that installing protrusions on the trailing side for low rotation number and installing dimples for comparatively large rotation number, was advantageous in terms of general results.

Shen et al. [4] proposed the heat transfer augmentation with orthogonal ribs, dimples or spherical protrusions in rotating and non-rotating channels. Mahmood et al. [5] simultaneously mounted dimples and protrusions on opposite sides of the channel and verified the increase in heat transfer via the cooling method of the compound devices. Lan et al. [6] used the compound cooling method and numerically studied thermal performance in a channel mounted with orthogonal rib-only, rib-dimple protrusions, or rib-spherical protrusions. They showed that the method of the rib-protrusion compound had the ability to enhance the heat transfer with lower pressure drop, and the protrusions

could also augment the rate of heat transfer similar to that of dimples with lower pressure loss.

Thus, a numerical simulation of a 3-dimensional hexagonal-dimpled channel flow is performed in the present work with the main goal of being visualized the changes in the flow structure and heat transfer patterns.

2. Dimpled-channel configuration

The flow system of interest is characterized by the staggered hexagonal dimples on the lower wall of a channel while the upper wall remains a smooth surface as depicted in Fig 1. The flow under consideration is expected to attain a periodical flow condition in which the velocity field repeats itself from one cell to another. The concept of periodically fully developed flow and its solution procedure was described in Ref. [7].

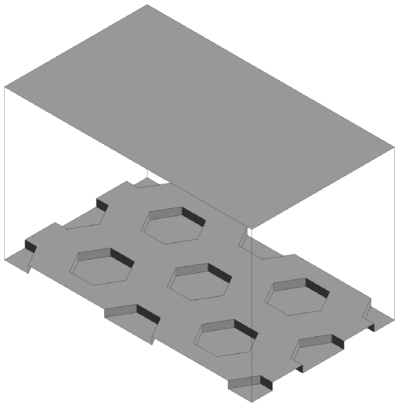

(a)

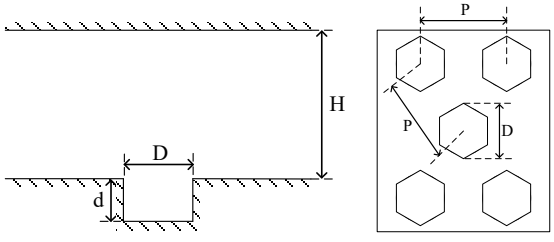

(b) (c)

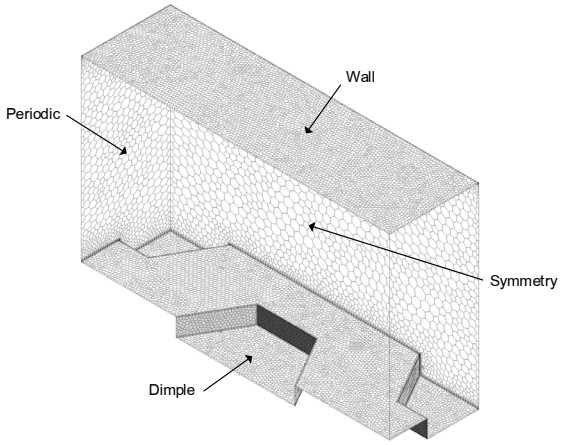

(d)

Fig. 1 (a) Hexagonal dimpled channel, (b) dimple geometry details, (c) staggered array of dimples, and (d) computational domain.

In the flow model, air enters the channel at inlet temperature, T_{in}=300 K. The geometrical parameters for the dimpled channel are the dimple diameter (D) =10 mm, channel height (H) =15 mm, dimple pitch (P) =15 mm, and dimple depth (d). In the present work, the relative dimple depth, d/H, is varied in a range of 0.03-0.20.

3. Computational details

The numerical model for fluid flow and heat transfer in a dimpled channel is developed under the following assumptions: steady three-dimensional turbulent and incompressible flow and heat transfer; constant fluid properties; and neglecting viscous dissipation, body forces and radiation heat transfer. Based on the above assumptions, the channel flow is governed by the Reynolds averaged Navier-Stokes (RANS) equations and the energy equation. In the Cartesian tensor system these equations can be written as follows:

Continuity equation:

$$\frac{\partial}{\partial x_i}(\rho u_i) = 0 \qquad (1)$$

Momentum equation:

$$\frac{\partial}{\partial x_j}(\rho u_i u_i) = -\frac{\partial p}{\partial x_i} + \frac{\partial}{\partial x_j}\left[\mu\left(\frac{\partial u_i}{\partial x_j} + \frac{\partial u_j}{\partial x_i}\right) - \rho\overline{u_i' u_j'}\right] \qquad (2)$$

where ρ is the density of fluid, and u_i is a mean component of velocity in the direction x_i , p is the pressure, μ is the dynamic viscosity, and u' is a fluctuating component of velocity. Repeated indices indicate summation from one to three for 3-dimensional problems.

Energy equation:

$$\frac{\partial}{\partial x_j}(\rho u_i T) = \frac{\partial}{\partial x_j}\left((\Gamma + \Gamma_t)\frac{\partial T}{\partial x_j}\right) \quad (3)$$

where Γ and Γ_t are molecular thermal diffusivity and turbulent thermal diffusivity, respectively and are given by

$$\Gamma = \frac{\mu}{Pr} \quad \text{and} \quad \Gamma_t = \frac{\mu_t}{Pr_t} \quad (4)$$

The Reynolds-averaged approach to turbulence modeling requires that the Reynolds stresses, $-\rho\overline{u_i'u_j'}$ in Eq. (2) needs to be modeled. The Boussinesq hypothesis relates the Reynolds stresses to the mean velocity gradients as seen in the equation below:

$$-\rho\overline{u_i'u_j'} = \mu_t\left(\frac{\partial u_i}{\partial u_j} + \frac{\partial u_j}{\partial u_i}\right) - \frac{2}{3}\left(\rho k + \mu_t\frac{\partial u_i}{\partial x_i}\right)\delta_{ij} \quad (5)$$

where k is the turbulent kinetic energy, defined by $k = \left(\frac{1}{2}\right)\overline{u_i'u_j'}$ and δ_{ij} is a Kronecker delta. The merit of the Boussinesq approach is the relatively low computational cost associated with the computation of the turbulent viscosity, μ_t given as $\mu_t = \frac{\rho C_\mu k^2}{\varepsilon}$. The RNG k–ε model is one of the two-equation models that employs the Boussinesq hypothesis and recommended for the internal-protruded dimple geometrics as found in Ref. [8].

The steady state transport equations are expressed as:

$$\frac{\partial}{\partial x_i}(\rho k u_i) = \frac{\partial}{\partial x_j}\left(\alpha_k \mu_{eff}\frac{\partial k}{\partial x_j}\right) + G_k - \rho\varepsilon \quad (6)$$

$$\frac{\partial}{\partial x_i}(\rho \varepsilon u_i) = \frac{\partial}{\partial x_j}\left(\alpha_\varepsilon \mu_{eff}\frac{\partial \varepsilon}{\partial x_j}\right) + C_{1\varepsilon}\frac{\varepsilon}{k}G_k - C_{2\varepsilon}\rho\frac{\varepsilon^2}{k} - R_\varepsilon \quad (7)$$

In the above equations, α_k and α_ε are the inverse effective Prandtl numbers for k and ε, respectively. $C_{1\varepsilon}$ and $C_{2\varepsilon}$ are constants. The effective viscosity μ_{eff} is written by

$$\mu_{eff} = \mu + \mu_t = \mu + \rho C_\mu \frac{k^2}{\varepsilon} \quad (8)$$

where C_μ is a constant and set to 0.0845, derived using the "renormalization group" (RNG) method.

All the governing equations were discretized by the SOU numerical scheme, coupling with the Coupled algorithm and solved using a finite volume approach [8]. For closure of the equations, the k-ε RNG turbulence model was utilized in the present study. The boundary conditions are as follows: no slip for all channel surfaces, constant heat flux for the lower surface and adiabatic for upper surface. The periodically fully developed condition was employed for the inlet and outlet section while symmetry was used for the left and right sides as depicted in Fig. 1(d). The solutions were converged when the normalized residual values were less than 10^{-5} for all variables but less than 10^{-9} only for the energy equation.

There are three parameters of interest in the present work, namely, Reynolds number (Re), friction factor (f) and Nusselt number (Nu). The Re is defined as

$$Re = \frac{(\rho \bar{u} D_h)}{\mu} \quad (9)$$

The f is computed by pressure drop, Δp across the channel length, L as

$$f = \frac{\left(\frac{\Delta p}{L}\right)D_h}{\left(\frac{1}{2}\right)\rho\bar{u}^2} \quad (10)$$

The local heat transfer is measured by local Nusselt number which can be written as

$$Nu_x = \frac{h_x D_h}{\lambda} \quad (11)$$

where λ is the thermal conductivity of air.

The area-average Nu can be obtained by

$$Nu = \frac{1}{A}\int Nu_x \, \partial A \quad (12)$$

The thermal enhancement factor (TEF) is defined as the ratio of the heat transfer coefficient of an augmented surface, h_a, to that of a smooth surface, h_0, at an equal pumping power and given by

$$\text{TEF} = \frac{h_a}{h_0}\Big|_{pp} = \frac{Nu/Nu_0}{(f/f_0)^{1/3}} \quad (13)$$

where Nu_0 and f_0 stand for Nusselt number and friction factor for the smooth channel, respectively.

4. Results and discussion

4.1 Verification of the smooth channel

Verification of the heat transfer and friction factor of the smooth channel is carried out by comparing to the Gnielinski and Petukhov correlations as shown in Figure 2. The present smooth channel result is seen to be in excellent agreement with data from Gnielinski and Petukhov correlations found in the open literature [8] for both the Nusselt number and the friction factor, less than 7 and 4 % deviation, respectively.

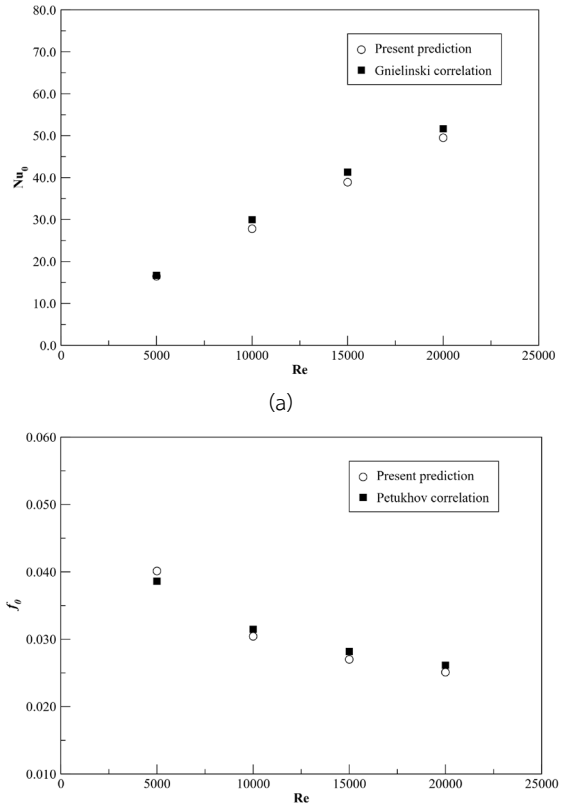

Fig. 2 Verification of (a) Nusselt number and (b) friction factor for smooth channel

4.2 Flow structure and heat transfer

Figure 3 shows the wall temperature variations and streamlines for d/H=0.03, 0.05, 0.10, 0.15, and 0.20 at Re = 10,000. It is observed in Fig. 3 that close to the downstream corners and downstream spanwise dimple edges, the smallest surface temperature regions are seen. Here, dimple-induced vortex structures encourage mixing and force cooler air from the main core of the channel into the wall-side regions. Similar trends are evident for d/H=0.10, 0.15 and 0.20, where low temperature regions are occasionally more spread out along the surface.

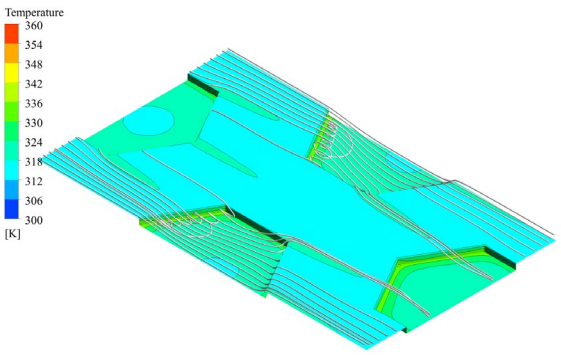

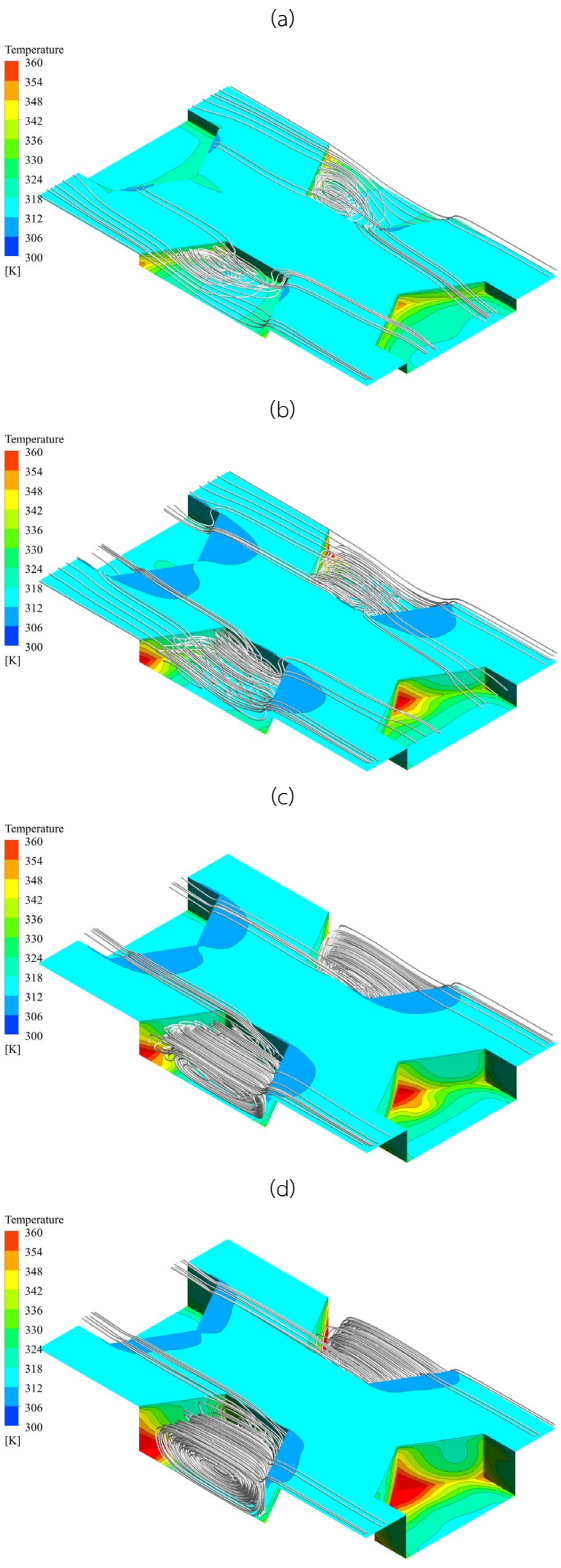

Fig. 3 Surface temperature contours and streamlines for (a) d/H=0.03, (b) d/H=0.05, (c) d/H=0.10, (d) d/H=0.15, and (e) d/H=0.20 at Re=10,000

Figure 4 shows local surface Nusselt number contours for d/H = 0.03, 0.05, 0.10, 0.15 and 0.20 at Re=10,000. For all h/H values, due to the flow separation and recirculation, the upstream dimple-half has the reduced heat transfer area, however the convective heat transfer areas in the downstream dimple-half and the downstream region of the dimple are significantly increased, especially areas behind the dimples, as the vortex flows from the dimples improve the turbulent flow mixing in the near-wall region considerably.

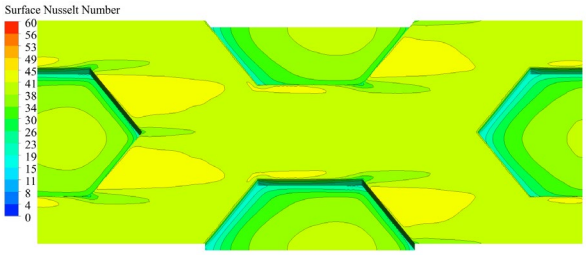

(a)

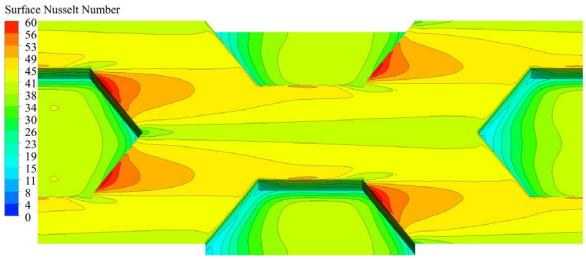

(b)

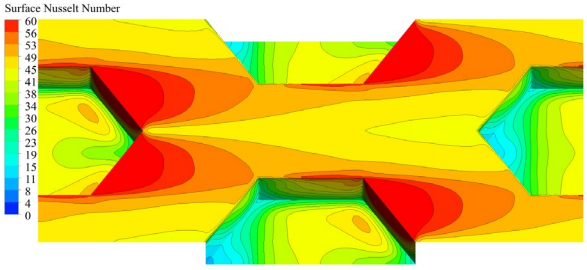

(c)

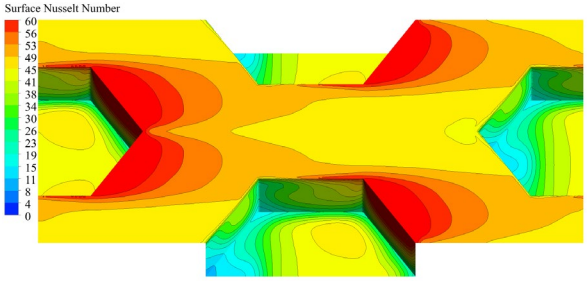

(d)

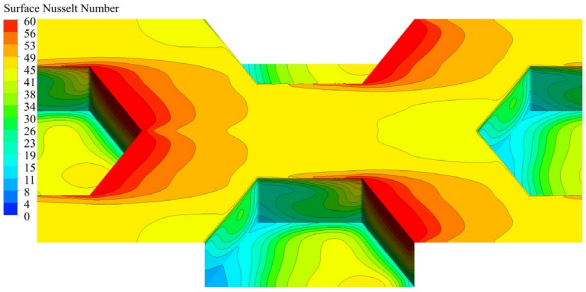

(e)

Fig. 4 Local Nusselt number contours on hexagonal dimple surface for (a) d/H=0.03, (b) d/H=0.05, (c) d/H=0.10, (d) d/H=0.15, and (e) d/H=0.20 at Re=10,000

4.3 Effect of hexagonal-dimple depth

The variations of Nusselt number ratio, Nu/Nu_0 and friction factor ratio, f/f_0 with Reynolds number (Re) for different d/H values are depicted in Figs 5(a) and 5(b), respectively. Nu/Nu_0 tends to decrease with the increase in Re. The d/H=0.10 provides the maximum Nu/Nu_0 around 1.52 at Re=10,000 where Nu/Nu_0 slightly increases for Re > 5,000 but shows a steep decrease for 10000< Re< 20,000.

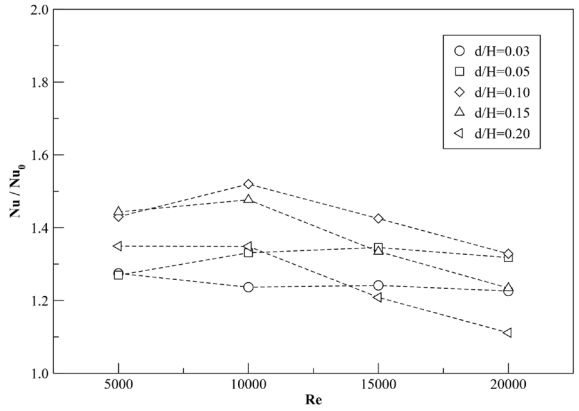

(a)

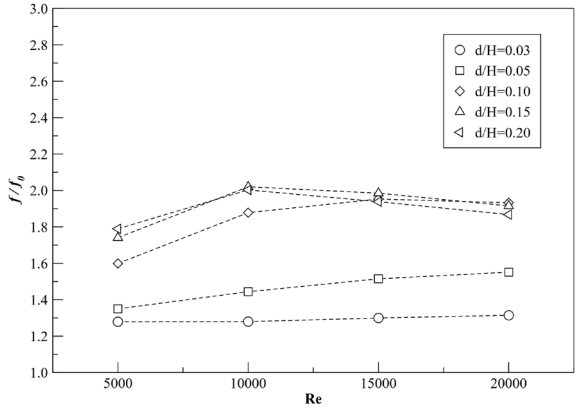

(b)

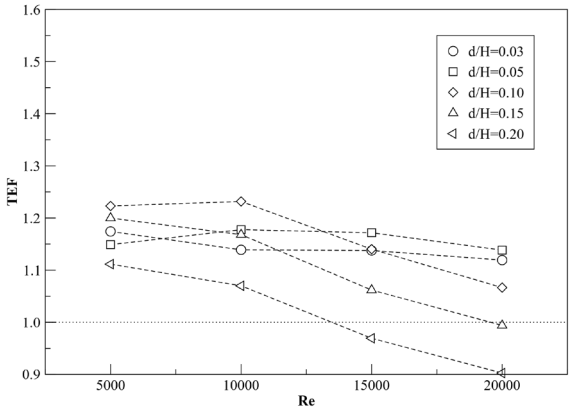

(c)

Fig. 5 Variations of (a) Nu/Nu_0, (b) f/f_0 and (c) TEF with Re

In general, the heat transfer augmentation is concerned with the pressure drop penalty in terms of increased friction factor. In Fig. 5(b), f/f_0 is seen to slightly increase with the increment of Re. The maximum f/f_0 of 2.02 is found at d/H=0.15 and Re=10,000.

Figure 5(c) shows the variation of thermal enhancement factor (TEF) with Re for airflow through the dimpled channel. In the figure, TEF of the dimple surface shows the downtrend with the rise in Re for various d/H values. It is visible that the dimple with d/H=0.10 has the highest TEF of 1.23 at Re=10,000. However, at Re=15,000, the d/H=0.05 yields the maximum TEF throughout. The TEF of the dimpled channel is seen to vary between 0.90 and 1.23, depending on d/H and Re values.

5. Conclusions

Turbulent flow and thermal characteristics have been studied numerically in a hexagonal dimpled channel. The vortex flow triggered by the hexagonal dimple helps cause impingement/attachment flows on the channel wall resulting in the higher heat transfer rate increase. The rate of heat transfer of the dimpled channel is about 1.11 to 1.52 times above the smooth channel. However, the increase in heat transfer is involved with the increased loss of friction ranging from 1.28 to 2.02 times the smooth channel. The dimpled channel has the thermal enhancement factor greater than unity and its peak value at d/H=0.10 and Re=10,000 is about 1.23, showing higher performance over the smooth channel.

6. References

[1] Ligrani, P.M., Oliveira, M.M. and Blaskovich, T. (2003). Comparison of heat transfer augmentation techniques. *AIAA J.*, vol. 41, pp. 337-372.

[2] Xia, G., Sunden, S. and Zhang, W. (2011). Comparisons of pins/dimples/protrusions cooling concepts for a turbine blade tip-wall at high Reynolds numbers. *J. Heat Transf.*, vol. 133.

[3] Elyyan, M.A. and Tafti, D.K. (2010). Effect of Coriolis forces in a rotating channel with dimples and protrusions, *Int. J. Heat Fluid Flow*, vol. 31, pp. 1–18.

[4] Shen, Z.Y., Xie, Y. and Zhang, D. (2015). Numerical predictions on fluid flow and heat transfer in U-shaped channel with the combination of ribs, dimples and protrusions under rotational effects. *Int. J. Heat Mass Transf.*, vol. 80, pp. 494–512.

[5] Mahmood, G.I., Sabbagh, M.Z. and Ligrani, P.M. (2001). Heat transfer in a channel with dimples and protrusions on opposite walls. *J. Thermophys. Heat Transf.*, vol. 15, pp. 273–283.

[6] Lan, J., Xie, Y. and Zhang, D. (2011). Heat transfer enhancement in a rectangular channel with the combination of ribs, dimples and protrusions. in: *Proceedings of ASME TURBO EXPO 2011*, Vancouver, Canada.

[7] Patankar, S.V., Liu, C.H. and Sparrow, E.M. (1977). Fully developed flow and heat transfer in ducts having streamwise-periodic variations of cross-sectional area, *ASME J. Heat Transfer*, vol. 99, pp. 180–186.

[8] Xie, G.N., Liu, J., Ligrani P.M. and Zhang, W. (2013). Numerical analysis of flow structure and heat transfer characteristics in square channels with internal-protruded dimple geometrics, *Int. J. Heat Mass Transfer*, vol. 67, pp. 81-97.